GOME OBSERVATIONS OF TROPOSPHERIC BRO

Andreas Richter, Folkard Wittrock, and John P. Burrows

Institute of Environmental Physics, University of Bremen, Germany
e-mail: Andreas.Richter@iup.physik.uni-bremen.de

ABSTRACT

Several years of data from the Global Ozone Monitoring Experiment (GOME) have been analysed for BrO absorptions. In both hemispheres, periods with locally enhanced BrO are observed throughout polar spring and are attributed to tropospheric BrO events. Most of the regions with enhanced BrO are located over sea ice and along the coasts of Antarctica and the Arctic Sea, confirming the model of bromine release from sea salt and activation on sea ice or snow. The seasonal variation and the observed columns are similar in both hemispheres indicating that similar mechanisms are operating in the Arctic and Antarctic. Comparable results have been obtained for 1995, 1996, 1997 and 1998, leading to the conclusion that enhanced tropospheric BrO is a typical feature of the polar troposphere in spring.

1. INTRODUCTION

Long-term observations of tropospheric ozone concentrations in polar regions have repeatedly shown periods of low ozone values in spring (refs 20, 4, 30). These "low ozone events" have been reported for both the Arctic and the Antarctic and are believed to be mostly of natural origin. Measurements of filterable bromine showed enhanced Br levels before and during such events (ref 3). More recently the presence of up to 30 pptv of BrO, an active form of bromine has been shown by long-path Differential Optical Absorption (DOAS) measurements (refs 13, 17). Ground-based zenith sky DOAS experiments have also provided evidence for periods of elevated tropospheric BrO in both Arctic (refs 31, 19) and Antarctic spring (ref 15). It now is widely accepted that catalytic cycles invoking BrO are responsible for the majority of the observed ozone losses, smaller contributions being proposed for cycles involving ClO and IO. Some recent modelling studies conclude that locally the rate of ozone loss is well explained assuming that sufficient halogen is present (ref 24). However, the sources of bromine in polar spring are not well understood. Two different sources have been proposed: organic bromine compounds like $CHBr_3$ (refs 3, 16) and sea salt aerosols ((refs 18, 29) and references therein).

With the Global Ozone Monitoring Experiment (GOME) instrument, BrO, one of the key species in polar spring tropospheric ozone depletion can for the first time be monitored globally. These measurements offer a unique opportunity to study the geographical and temporal evolution of the low ozone events and contribute to the continuing search for the sources and mechanisms of bromine release in the polar troposphere.

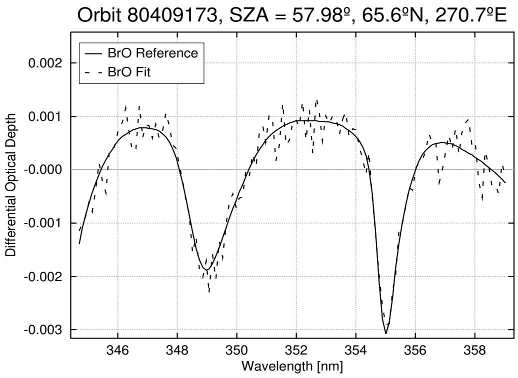

Figure 1. Example of a BrO fit during a tropospheric BrO event. The solid line is the scaled laboratory reference, the dotted line the fit result.

2. DATA ANALYSIS

The GOME is a UV/VIS double monochromator with a spectral range of 240–793 nm and a resolution of 0.2 nm (< 400 nm) and 0.4 nm (> 400 nm). GOME observes the light scattered from the earth's atmosphere and reflected by the ground in near nadir viewing geometry. It operates on board of ERS-2 which is on a sun-synchronous orbit since April 1995. The spatial resolution of GOME is 40×320 km^2 for solar zenith angles (SZA) below 86°. Global coverage is achieved within 3 days at the equator and within 1 day at a latitude of 67°.

The main objective of the GOME instrument is the global measurement of vertical columns of O_3 and NO_2. However, other trace gases including H_2O, SO_2, OClO and HCHO can be retrieved by means of the DOAS technique (ref 7). After the first detection of BrO in GOME measurements (ref 9), several studies of stratospheric and tropospheric BrO from GOME have been performed (refs 14, 27, 22, 8).

In this study, GOME data have been analysed for BrO using the well known DOAS technique developed for ground-based measurements. Calibrated earth shine and solar irradiance spectra were used as provided by ESA through DLR-DFD. In order to get the best spatial resolution, only the three forward scans have been included, limiting the available range of solar zenith angles to values below 86°.

2.1. Spectral fitting

For the BrO retrieval, a spectral fitting window of 344.7 – 359 nm was selected. This spectral range is similar to that used for the ground-based measurements (ref 10) and was chosen to provide large differential BrO signals and small interference from other absorbers. In the fit, the absorption cross-sections of BrO (ref 28), O_4 (ref 11), NO_2 (ref 5) and O_3 (ref 6) at 221 and 241 K have been used together with a synthetic Ring spectrum (ref 26) compensating the effect of Raman scattering in the atmosphere. The wavelength calibration of BrO has been corrected by +0.17 nm as suggested by (ref 2) and recently confirmed by FTS measurements in Bremen (*O. Fleischmann, private communication*). After cross-calibration with the FTS measurements of (ref 25), both O_3 and NO_2 cross-sections have been shifted by +0.03 nm to correct for an error in wavelength calibration.

The slit function of channel 2 of the GOME instrument is to narrow for sufficient sampling of the spectra with the diode array used as detector. Due to a small doppler shift, GOME earth-shine and direct sun measurements have a systematic difference of approximately 0.008 nm in the wavelength sampling. In addition, small thermal drifts of the instrument calibration have to be corrected in the fit. Therefore, interpolation of the earth-shine spectra is necessary for the analysis, leading to large residuals from undersampling errors. This can be accounted for by either averaging over adjacent spectral points and thereby reducing the undersampling or by fitting a simulated undersampling spectrum as suggested by (ref 8). In this study, an undersampling spectrum and no smoothing were used. One example of a BrO fit result is shown in figure 1. The BrO slant column for this particular pixel is $4.25 \cdot 10^{14}$ molec/cm^2, this large value being attributed to a tropospheric BrO event. For the plot, an averaged residual has been included in the fit to compensate for constant instrument effects. This reduces the residuals but has negligible influence on the retrieved BrO columns. It therefore has not been used in the analysis discussed below.

2.2. Airmass factors

The DOAS fit results are slant columns, i.e., the integral of the absorber concentration along the line of sight. To convert slant into vertical columns, airmass factors (AMFs) have been computed with the radiative transfer model GOMETRAN (ref 23).

2.2.1. Stratospheric airmass factors For solar zenith angles below 70°, the AMF is essentially independent of the assumed vertical profile of the absorber. However, at larger SZA significantly different airmass factors result from different profiles as shown in figure 2. The profiles used for the calculations were taken from two BrO measurements of (ref 12), one at high latitudes in February and one in mid-latitudes in November. Little is known about the latitudinal and seasonal changes of stratospheric BrO profiles. Therefore, the same airmass factor (based on the high latitude profile of (ref 12)) has been used for all latitudes and seasons. Assuming that the two profiles used in figure 2 are extreme cases, the maximum error introduced from the use of a constant airmass factor is of the order of 10% for GOME measurements below 86° SZA.

2.2.2. Tropospheric airmass factors In the wavelength region used for BrO retrieval, a significant part of the

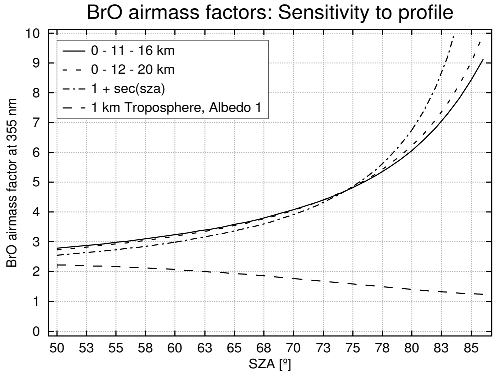

Figure 2. Airmass factors for different vertical BrO profiles. All values are for 355 nm. The two stratospheric profiles have been adapted from (ref 12) and are zero below the tropopause at 11 (12) km, increase linearly to 16 (20) km and are constant above that height.

photons measured by GOME are scattered in the upper troposphere and do not penetrate the atmosphere to the ground. This is particularly true for situations with low albedo, where photons reflected from the ground are only a small contribution to the overall intensity of the earth-shine spectrum. As a result, airmass factors for tropospheric absorbers depend strongly on the albedo as shown in figure 3. For an absorber layer in the lowest 1000 m of the atmosphere, the airmass factor at high sun increases from 0.25 to 2.25 for a change of albedo from 0 to 1. This implies, that GOME measurements in the UV are much more sensitive to tropospheric absorbers above ice than above open water. For solar zenith angles below 50°, the tropospheric and stratospheric airmass factors are of the same magnitude. For lower sun, the sensitivity towards tropospheric absorptions decreases significantly while at the same time the stratospheric airmass factor increases (fig. 2). This implies that tropospheric absorbers are difficult to detect with GOME at low sun (high latitudes in spring, autumn and winter).

2.2.3. Separation of stratosphere and troposphere The BrO slant columns measured with GOME are the sum of both tropospheric and stratospheric columns, weighted with different airmass factors. As BrO is not a strong absorber, the GOME measurements themselves contain not enough information to determine the vertical profile of the molecule.

There are however several arguments which give strong support to the interpretation of the large BrO absorptions as tropospheric events:

- On several occasions, GOME observations of high BrO columns coincide with ground-based measurements of enhanced tropospheric BrO (see *Wittrock et al.* and *Wagner et al.*, this issue for a more detailed validation of GOME BrO measurements).
- The large BrO absorptions coincide with low cloud cover fraction
- Many of the observed BrO events are strongly localised and not associated to the movements of the

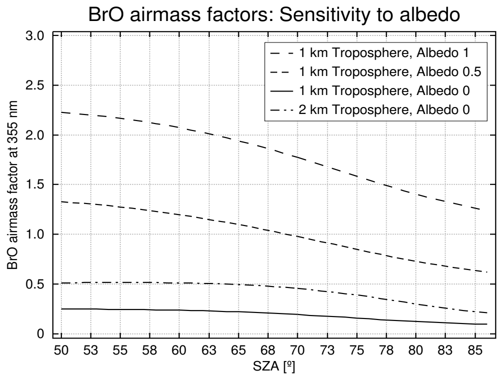

Figure 3. Sensitivity of tropospheric airmass factors to changes in albedo and profile height. All airmass factors are at 355 nm, nadir viewing geometry and include multiple scattering.

polar vortex.

- Assuming a stratospheric origin of the observed BrO peaks would imply stratospheric mixing ratios of more than 30 ppt in some cases, inconsistent with previous measurements and model predictions.

In order to determine the tropospheric BrO column, the stratospheric column has to be estimated and subtracted from the measured signal. Estimates of the stratospheric column can be based on other GOME measurements assuming temporal and/or spatial homogeneity of the stratospheric BrO (ref 22) or from model predictions. Clearly, both approaches can lead to large errors in the derived tropospheric values. In this study, no attempt was made to separate tropospheric and stratospheric columns. Tropospheric BrO events are identified by the magnitude of the total column and stratospheric airmass factors used. Therefore, all plots should be interpreted in a qualitative way only.

2.3. Error discussion

Several error sources have to be considered for the accuracy of the GOME BrO columns: instrumental errors, systematic analysis errors and errors in the airmass factors. Two methods have been used to estimate the random error in the BrO slant columns: the statistical error as determined from the fit and the difference between the three forward scans and the following back scan that covers approximately the same area. Both approaches result in similar values of an absolute error in the BrO slant column of less than $3 \cdot 10^{13}$ molec/cm^2 for an individual pixel.

The main systematic error source in the DOAS fit is the uncertainty in the BrO cross section, which is in the order of 20%. In addition, there are other, smaller error sources like stratospheric temperature changes, the I_0-effect or errors in the wavelength calibration that are discussed in detail in (ref 1). As discussed above, both stratospheric and tropospheric airmass factors for BrO depend on the assumed scenario. In addition, the weighting between tropospheric and stratospheric airmass factor depends on the cloud fraction. Without accurate values for albedo, aerosol loading, cloud fraction and vertical profile of the absorber, uncertainties in airmass factors can exceed 50% and will dominate the total error of the tropospheric BrO columns.

Additional errors arise in the determination of the tropospheric BrO column. As the stratospheric contribution has to be subtracted from the total columns, any error in the estimation of the stratospheric BrO results in an error in the tropospheric column. Local changes in the stratospheric column (resulting for example from changes in tropopause height) can potentially be misinterpreted as tropospheric BrO enhancements.

3. RESULTS AND DISCUSSION

In this study, several years of GOME BrO data have been analysed in the regions poleward of 40° in both hemispheres. To facilitate the discussion of the temporal and spatial behaviour of the tropospheric BrO, monthly averages of vertical BrO columns have been derived. For the conversion from slant to vertical columns, airmass factors based on the high latitude profile described in section 2.2.1 have been used independent of season and latitude. As discussed above, the resulting error is in the order of 10% for stratospheric BrO, but much larger for the tropospheric columns.

3.1. Northern hemisphere

In figure 4, BrO vertical columns in the northern hemisphere are shown for February to July 1998. On average, GOME measures a vertical column of about $6 \cdot 10^{13}$ molec/cm^2 in February and $4 \cdot 10^{13}$ molec/cm^2 in July. This is in good agreement with values from zenith-sky measurements (ref 21), but clearly in excess of model estimates for the stratosphere and the integrated columns from balloon borne measurements. This discrepancy between total and stratospheric columns has prompted the hypothesis of a significant BrO background concentration in the upper troposphere (see *Pfeilsticker et al.*, this issue). However, up to now no direct evidence was found for such a tropospheric BrO layer.

3.1.1. Seasonal variation

Starting in late February, localised regions with enhanced BrO columns appear in the GOME data. Most of these measurements are in the Hudson Bay area and along the coastlines of the Arctic Ocean, but in April and May high values are also detected over the arctic ice. The last such events are observed in early June and do not reappear for the rest of the year.

Individual BrO events usually extend over several hundred kilometres and disappear after a few days. This is in agreement with ground-based measurements in Ny-Ålesund showing episodes of high BrO in connection with rapid boundary layer ozone destruction and very low O_3 values for periods of hours to days. However, GOME data show that in some areas the frequency of BrO events is much higher than in Ny-Ålesund or Greenland. In fact, as shown in figure 4, BrO columns along the cost of the Arctic Sea are enhanced by a factor of 1.5 in the monthly

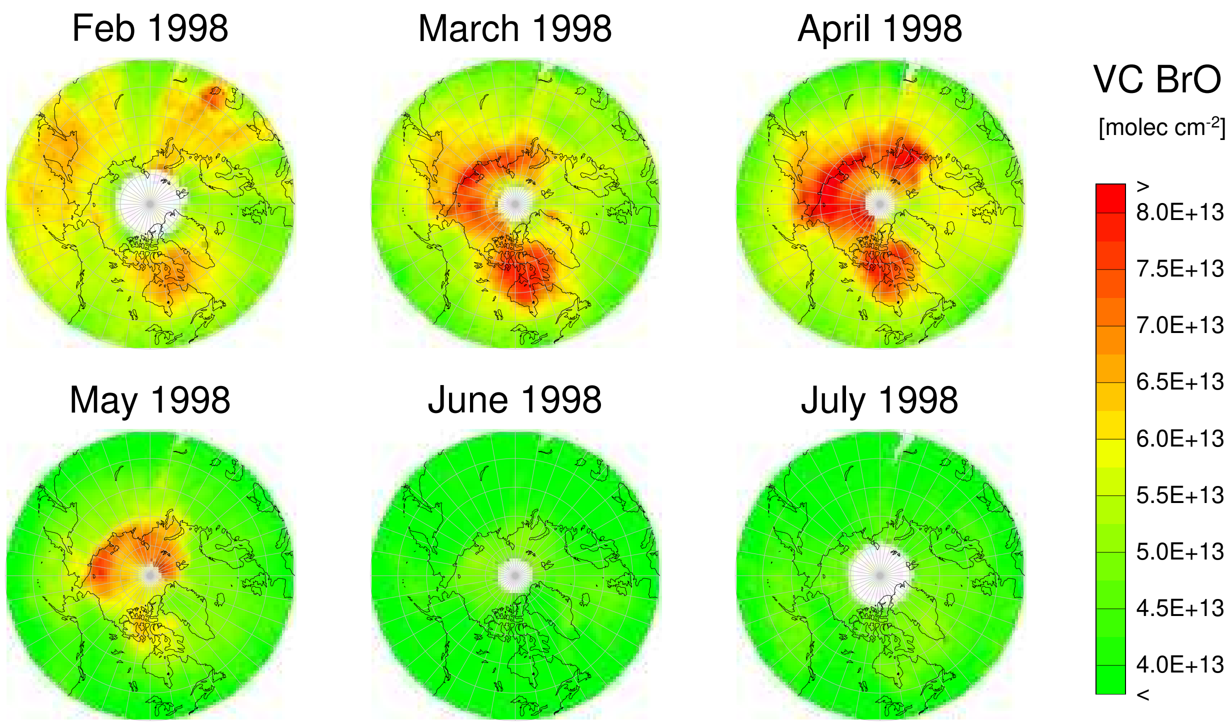

Figure 4. Monthly averages of GOME BrO in the northern hemisphere. Vertical columns have been derived using an airmass factor appropriate for stratospheric BrO. Therefore, tropospheric BrO columns are underestimated at high latitudes.

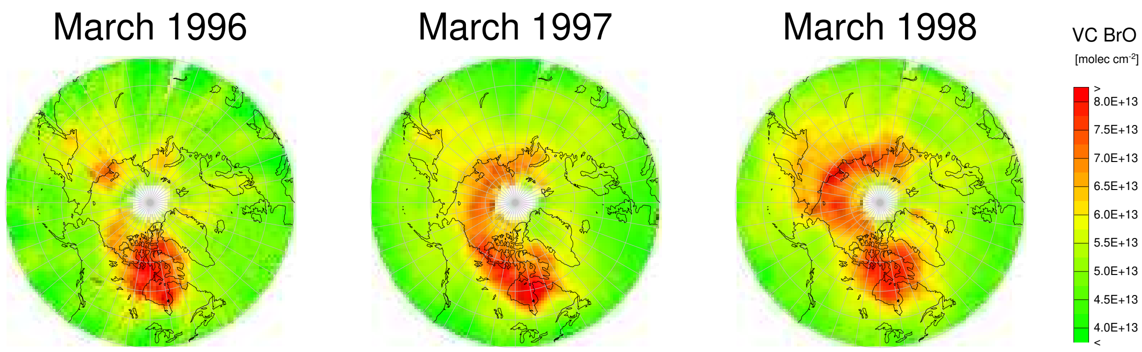

Figure 5: Monthly averages of GOME BrO in the northern hemisphere.

average, indicating the large impact of the BrO events on boundary layer chemistry in the Arctic spring.

Most of the observed BrO events are located near the coast or over the ice cap. This supports the assumption, that bromine is released from sea-salt and that sea-ice (or the snow covering the ice) is involved in bromine activation. Tropospheric BrO events observed by GOME seem to move northwards from February to May, in agreement with the assumption that ice with some cracks is necessary to release bromine. However, as the solar zenith angle increases with season, GOME sensitivity towards tropospheric BrO increases and this could explain part of the observed trend.

3.1.2. Year to year variation In fig. 5, BrO vertical columns are shown for March 1996, 1997 and 1998. As can be seen from the plot, the general pattern and absolute values of the BrO events is comparable from year to year. There are however differences in the number and distribution of the events, which for example were much less frequent along the Russian coast in March 1996 than in 1998. Possible reasons for the differences from year to year are changes in temperature and sea ice cover, but cloudiness is also a factor for measurements from space.

3.2. Southern hemisphere

In figure 6, monthly averages of GOME BrO columns are shown for the southern hemisphere from August 1997 to January 1998. From August to November, BrO events occur frequently in a ring around the Antarctic continent. In late November and December, some periods of enhanced BrO columns are also observed over the Antarctic continent near parts of the coast where the ice breaks up

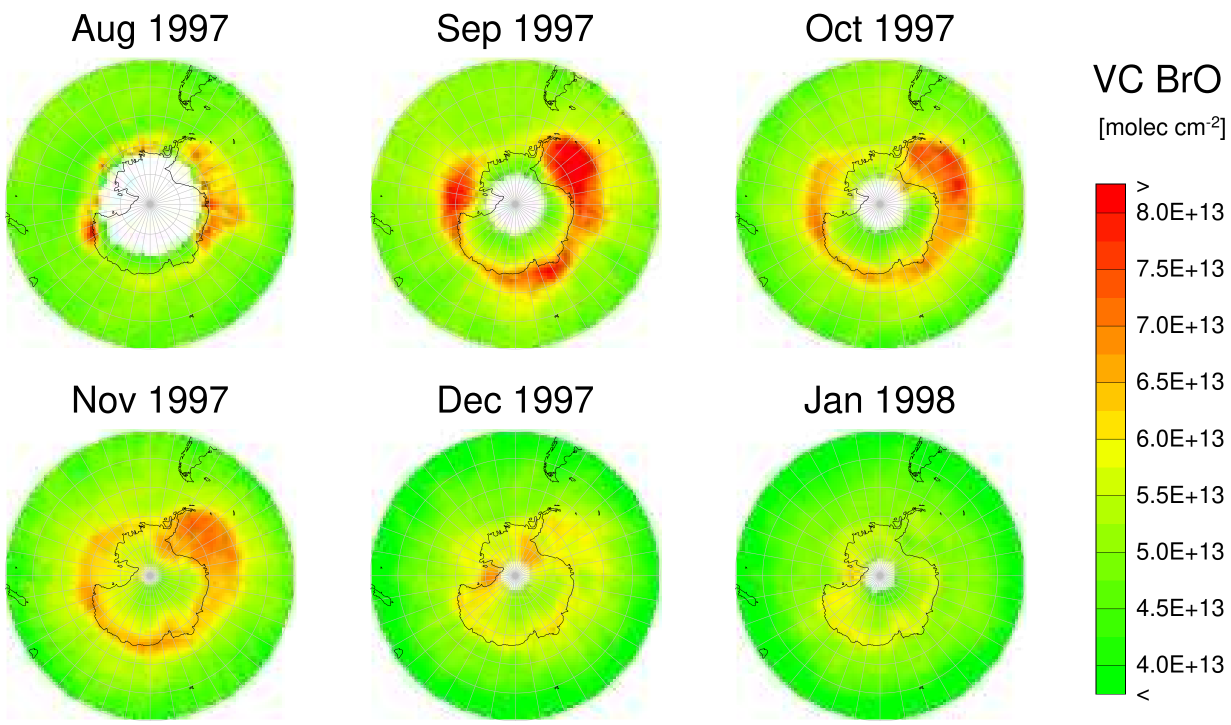

Figure 6. Monthly averages of GOME BrO in the southern hemisphere. Vertical columns have been derived using an airmass factor appropriate for stratospheric BrO. Therefore, tropospheric BrO columns are underestimated at high latitudes.

early. The ring structure of the enhanced BrO explains the small number of tropospheric BrO events observed from ground-based measurements on Antarctica - obviously most of these events are located over the ice. The strong correlation between sea-ice coverage and BrO enhancements is shown in figure 7, where BrO and reflected intensity in the southern hemisphere are compared for September 1995, 1996 and 1997. The intensity of the GOME earth-shine spectra has been averaged over the wavelength interval used for the BrO fit and corrected for the cosine response. In a monthly average, cloud influences are smoothed out and reflectivity gives a good idea of ice coverage. A striking correlation exists between intensity and BrO columns, indicating that BrO enhancements are constrained to the ice covered region. This is similar to the observations in the northern hemisphere and again confirms the model of bromine release over sea ice. However, the pronounced sensitivity of tropospheric airmass factors to changes in albedo can clearly influence this result. If present, BrO events over water would lead to much smaller BrO slant columns than comparable events over ice.

3.3. Comparison of the hemispheres

Both the seasonal variation and the column amounts of the tropospheric BrO in the two hemispheres are comparable. The differences in sea-land distribution are reflected in the spatial pattern of the BrO events and with the exception of the Hudson Bay area, the bulk of the BrO in the northern hemisphere is closer to the pole than in the southern hemisphere. Most of the BrO is observed over sea ice and along the coasts of the continents. The similarity of the BrO distribution in the two hemispheres is an indication that similar chemical and physical processes are involved in the bromine activation in arctic and antarctic spring.

4. SUMMARY AND CONCLUSIONS

Several years of data from the GOME satellite instrument have been analysed for BrO absorptions. Stratospheric BrO columns show a small seasonal variation with a maximum of $6{\cdot}10^{13}$ molec/cm^2 during winter at high latitudes and about $4 \cdot 10^{13}$ molec/cm^2 in summer. Superimposed on the stratospheric columns are events of large BrO enhancements attributed to tropospheric BrO. These events start in early spring and continue for 4 months, both in the southern and in the northern hemisphere. Most BrO enhancements are observed over sea ice and along the coasts of Antarctica and the Arctic Sea. The general pattern is similar in 1995, 1996, 1997 and 1998, but differences in the frequency and the spatial distribution of the events exist, probably because of differences in temperature, sea-ice and cloud coverage.

The presented GOME observations agree well with ground-based observations of sporadic BrO events at coastal stations and continuous O_3 depletion over the arctic ice. The distribution of the BrO enhancements supports the model of bromine release from sea salt and a role of sea-ice in the activation of the bromine. The similarities between the two hemispheres indicate that the same mechanisms could be responsible for the bromine release in the Arctic and Antarctic. From the GOME

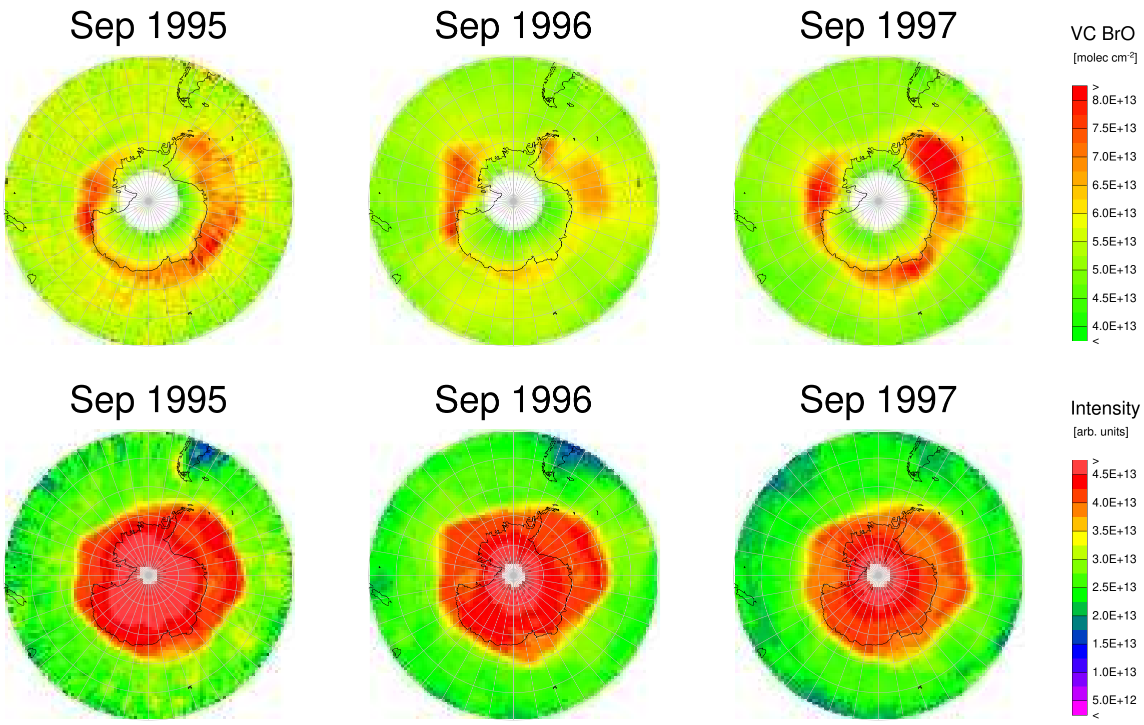

Figure 7. Monthly averages of GOME BrO and Reflectivity in the southern hemisphere. Averaged reflectivity can be used as a proxy for sea-ice coverage. Measurements in 1995 were subject to instrumental problems and noisier than in the following years.

data it appears, that enhanced BrO concentrations are not sporadic events in the polar boundary layer, but rather a frequent and common feature of polar spring. The presence of these large halogen amounts in the lower atmosphere at high latitudes should have a strong impact on tropospheric chemistry in the polar regions and could possibly also be important for mid-latitudes.

ACKNOWLEDGMENTS

The authors would like to thank M. Vountas for the preparation of the synthetic Ring spectrum. Helpful discussions with T. Wagner, H. Harder and M. Eisinger are gratefully acknowledged. GOME data have been supplied by the German Aerospace Centre / DLR. Parts of this work have been funded by the University of Bremen, the European Union and the German Space Agency (DARA).

REFERENCES

1. S. R. Aliwell, P. V. Johnston, A. Richter, M. Van-Roozendael, T. Wagner, D. W. Arlander, J. P. Burrows, D. J. Fish, R. L. Jones, K. Karlsen-Tornkvist, J. C. Lambert, K. Pfeilsticker, and I. Pundt. Analysis for BrO in zenith-sky spectra - an intercomparison exercise for analysis improvement. *to be submitted to J. Geophys. Res.*, 1999.

2. S. R. Aliwell, R. L. Jones, and D. J. Fish. Mid-latitude observations of the seasonal variation of BrO. 1. Zenith-sky measurements. *Geophys. Res. Lett.*, 24:1195–1198, 1997.

3. L. A. Barrie, J. W. Bottelsheim, R. C. Schnell, P. J. Crutzen, and R. A. Rasmussen. Ozone destruction and photochemical reactions at polar sunrise in the lower Arctic atmosphere. *Nature*, 334:138–141, 1988.

4. J. W. Bottenheim, A. G. Gallant, and K. A. Brice. Measurements of NO_y species and O_3 at 82°N latitude. *Geophys. Res. Lett.*, 22:599–602, 1986.

5. J. P. Burrows, A. Dehn, B. Deters, S. Himmelmann, A. Richter, S. Voigt, and J. Orphal. Atmospheric remote-sensing reference data from GOME: Part 1. Temperature-dependent absorption cross-sections of NO_2 in the 231–794 nm range,. *J. Quant. Spectrosc. Rad. Transfer*, 60:1025–1031, 1998.

6. J. P. Burrows, A. Richter, A. Dehn, B. Deters, S. Himmelmann, S. Voigt, and J. Orphal. Atmospheric remote-sensing reference data from GOME: Part 2. Temperature-dependent absorption cross-sections of O_3 in the 231–794 nm range,. *J. Quant. Spectrosc. Rad. Transfer*, 61:509–517, 1999.

7. J. P. Burrows, M. Weber, M. Buchwitz, V. Rozanov, A. Ladstätter-Weißenmayer, A. Richter, R. DeBeek, R. Hoogen, K. Bramstedt, K. U. Eichmann, M. Eisinger, and D. Perner. The Global Ozone Monitoring Experiment (GOME): Mission Concept and First Scientific Results. *J. Atmos. Sci.*, 56:151–175, 1999.

8. K. Chance. Analysis of BrO measurements from the Global Ozone Monitoring Experiment. *Geophys. Res. Lett.*, 25:3335–3338, 1998.

9. M. Eisinger, J. P. Burrows, and A. Richter. Studies on the precision of GOME irradiance and radiance products and GOME measurements of OClO and BrO over Antarctica. *GOME Geophysical Validation Campaign. Final results workshop proceedings*, 1996.

10. M. Eisinger, A Richter, Burrows Ladstätter-Weißenmayer, and J. P. DOAS zenith sky observations: 1. BrO measurements over Bremen (53°N) 1993-1994. *J. Atm. Chem.*, 25:93–108, 1997.

11. G. D. Greenblatt, J. J. Orlando, J. B. Burkholder, and A. R. Ravishankara. Absorption measurements of oxygen between 330 and 1140 nm. *J. Geophys. Res.*, 95:18577–18582, 1990.

12. H. Harder, C. Camy-Peyret, F. Ferlemann, R. Fitzenberger, T. Hawat, and H. Osterkamp. Stratospheric BrO Profiles Measured at Different Latitudes and Seasons: Atmospheric Observations. *Geophys. Res. Lett.*, 25:3843–3846, 1998.

13. M. Hausmann and U. Platt. Spectroscopic measurement of bromine oxide and ozone in the high Arctic during Polar Sunrise Experiment 1992. *J. Geophys. Res.*, 99:25399–25413, 1994.

14. E. Hegels, P. J. Crutzen, T. Klüpfel, D. Perner, and J. P. Burrows. Global distribution of atmospheric bromine oxide from GOME on the earth observing satellite ERS-2. *Geophys. Res. Lett.*, 25:3127–3130, 1998.

15. K. Kreher, P. V. Johnston, S. W. Wood, B. Nardi, and U Platt. Ground-based measurements of tropospheric and stratospheric BrO at Arrival Heights, Antarctica. *Geophys. Res. Lett.*, 24:3201–3024, 1997.

16. G. LeBras and U. Platt. A possible mechanism for combined chlorine and bromine catalyzed destruction of tropospheric ozone in the arctic. *Geophys. Res. Lett.*, 22:599–602, 1995.

17. M. Martinez-Walter, T. Arnold, D. Perner, R: Seuwen, and F: Stordal. The role of halogen oxides and peroxy radicals in the boundary layer during arctic ozone depletion 1995/1996. *Proceedings of XVIII Ozone Symposium in L'Aquila*, 1996.

18. J. C. McConnell, G. S. Henderson, L. Barrie, J. Bottenheim, H. Niki, C. H. Langford, and E. M. J. Templeton. Photochemical bromine production implicated in Arctic boundary-layer ozone depletion. *Nature*, 355:150–152, 1992.

19. H. L. Miller, A. Weaver, R. W. Sanders, K. Arpag, and S. Solomon. Measurements of Artic sunrise surface ozone depletion events at Kangerlussuaq, Greenland (67°N, 51°W). *Tellus*, 49, 1997.

20. S. J. Oltmans and W. D. Komhyr. Surface ozone distributions and variations from 1973-1984 Measurements at the NOAA Geophysical Monitoring for Climatic Change Baseline Observatories. *J. Geophys. Res.*, 91:5229–5236, 1986.

21. A. Richter, M Eisinger, Burrows Ladstätter-Weißenmayer, and J. P. DOAS zenith sky observations. 2. Seasonal variation of BrO over Bremen (53°N) 1994-1995,. 1998. J. Atm. Chem., in press.

22. A. Richter, F. Wittrock, M. Eisinger, and J. P. Burrows. GOME observations of tropospheric BrO in Northern Hemispheric spring and summer 1997. *Geophys. Res. Lett.*, 25:2683–2686, 1998.

23. V. Rozanov, D. Diebel, R. J. D. Spurr, and J. P. Burrows. GOMETRAN: A radiative transfer model for the satellite project GOME - the plane parallel version. *J. Geophys. Res.*, 102:16683, 1997.

24. R. Sander, R. Vogt, G. W. Harris, and P. J. Crutzen. Modeling the chemistry of ozone, haolgen compounds, and hydrocarbons in the arctic troposphere during spring. *Tellus*, 49:523–532, 1997.

25. S. Voigt. Hochauflösende Fourier-Transform-Spektroskopie atmosphärischer Spurengase im ultravioletten, sichtbaren und nahinfraroten Spektralbereich: CO, NO_2 und O_3. *PhD thesis, University of Bremen*, 1998.

26. M. Vountas, V. V. Rozanov, and J. P. Burrows. Ring effect: Impact of rotational Raman scattering on radiative transfer in earth's atmosphere. *J. Quant. Spectrosc. Radiat. Transfer*, 60:943–961, 1998.

27. T. Wagner and U. Platt. Satellite mapping of enhanced BrO concentrations in the troposphere. *Nature*, 395:486–490, 1998.

28. A. Wahner, A. R. Ravishankara, S. P. Sander, and R. R. Friedl. Absorption cross section of BrO between 312 and 385 nm at 298 K and 223 K. *Chemical Physics Letters*, 152:507–512, 1988.

29. S. Wessel. Tropospheric ozone variations in polar regions. *Berichte zur Polarforschung*, 1997.

30. P. Winkler, S. Brylka, and D. Wagenbach. Regular fluctuations of surface ozone at Georg-von-Neumayer-Station, Antarctica. *Tellus*, 44:33–40, 1992.

31. F. Wittrock, M. Eisinger, A. Ladstätter-Weißenmayer, A. Richter, and J. P. Burrows. Ground-based UV/vis measurements of O_3, NO_2, BrO and OClO over Ny-Ålesund, 78°N. *Proceedings of XVIII Ozone Symposium in L'Aquila*, 1996.